Provided for non-commercial research and education use.
Not for reproduction, distribution or commercial use.

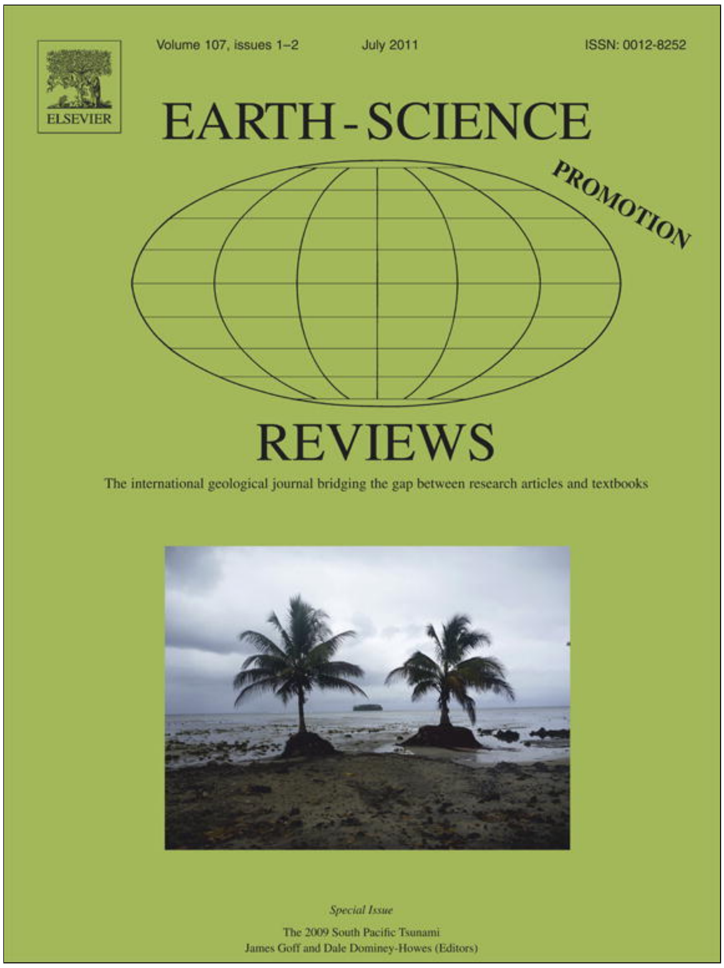

This article appeared in a journal published by Elsevier. The attached copy is furnished to the author for internal non-commercial research and education use, including for instruction at the authors institution and sharing with colleagues.

Other uses, including reproduction and distribution, or selling or licensing copies, or posting to personal, institutional or third party websites are prohibited.

In most cases authors are permitted to post their version of the article (e.g. in Word or Tex form) to their personal website or institutional repository. Authors requiring further information regarding Elsevier's archiving and manuscript policies are encouraged to visit:

http://www.elsevier.com/copyright

Author's personal copy

Earth-Science Reviews 107 (2011) 76–90

Contents lists available at ScienceDirect

Earth-Science Reviews

journal homepage: www.elsevier.com/locate/earscirev

The use of boulders for characterising past tsunamis: Lessons from the 2004 Indian Ocean and 2009 South Pacific tsunamis

Samuel Etienne [a,b,*], Mark Buckley [c], Raphaël Paris [b], Aruna K. Nandasena [d], Kate Clark [e], Luke Strotz [f], Catherine Chagué-Goff [f,g], James Goff [f], Bruce Richmond [c]

[a] Université de la Polynésie française, BP 6590, Faa'a, Tahiti, French Polynesia
[b] CNRS, UMR6042 GEOLAB, M.S.H., 4 rue Ledru, 63057 Clermont-Ferrand cedex 1, France
[c] U.S. Geological Survey, 400 Natural Bridges Drive, Santa Cruz, CA 95060, USA
[d] Graduate School of Science and Engineering, Saitama University, 255 Shimo-okubo, Sakura-ku, Saitama, 338-8570, Japan
[e] GNS Science, PO Box 30368, Lower Hutt, New Zealand
[f] Australian Tsunami Research Centre, University of New South Wales, Sydney 2052, NSW, Australia
[g] Australian Nuclear Science and Technology Organisation, Locked Bag 2001, Kirrawee DC, NSW, 2232 Australia

ARTICLE INFO

Article history:
Received 19 July 2010
Accepted 29 December 2010
Available online 6 January 2011

Keywords:
boulder deposit
tsunami
Samoa
Indonesia
geomorphology
transport simulation

ABSTRACT

Tsunamis are high energy events capable of transporting extremely heavy loads including boulders. We compare boulder deposits created by two modern tsunami events, the 2004 Indian Ocean and the 2009 South Pacific tsunamis, where the boulder sources were in similar topographic settings, and for which we have accurate data on the wave characteristics. Boulder distribution, preferential orientation and numerical simulation of boulder transport are discussed. A comparison between the impacts of the South Pacific and Indian Ocean tsunamis shows similar characteristics, such as limited landward extent and the absence of landward fining. Differences between the results from modelling and field data are most probably caused by variables such as coastal plain roughness (buildings, trees), microtopography, particle shape, and boulder collision during transport that are summarised as coefficients in the mathematical models. Characterising modern events through coarse sediment deposits provides valuable information to help identify and interpret palaeo-tsunami imprints on coastal landscapes.

© 2011 Elsevier B.V. All rights reserved.

Contents

* Corresponding author. Université de la Polynésie française, BP 6590, Faa'a, Tahiti, French Polynesia.
E-mail address: samuel.etienne@upf.pf (S. Etienne).

0012-8252/$ – see front matter © 2011 Elsevier B.V. All rights reserved.
doi:10.1016/j.earscirev.2010.12.006

Author's personal copy

1. Introduction

Coastal boulders of marine origin in unglaciated environments represent an unusual sediment class because their transport is restricted to high-energy events such as cyclones (Morton et al., 2006; Richmond and Morton, 2007; Terry, 2007), extra-tropical storms (Hansom and Hall, 2009; Etienne and Paris, 2010), swells induced by low pressure systems (Laboute, 1985; Smith et al., 2010), or tsunamis (e.g. Dawson, 1994; Paris et al., 2009). They are typically found in six different morphological situations and sedimentary assemblages: *mega-blocks* on coastal platforms (e.g. Bourrouilh-Le Jan and Talandier, 1985; Hearty, 1997; Noormets et al., 2002; Kelletat et al., 2004; Scheffers, 2005; Frohlich et al., 2009); *boulder beaches* (Oak, 1984; McKenna, 1990; Etienne and Paris, 2010; Richmond et al., in press); *cliff-top boulders* (e.g. Williams and Hall, 2004; de Lange et al., 2006; Goff et al., 2006a; Hall et al., 2006; Hall et al., 2008; Suanez et al., 2009; Etienne and Paris, 2010; Richmond et al., in press); *fields of scattered boulders and boulder clusters* (e.g. Shi et al., 1995; Mastronuzzi and Sansò, 2000, 2004; Whelan and Kelletat, 2005; Goff et al., 2006b; Scicchitano et al., 2007; Scheffers and Scheffers, 2007; Goto et al., 2010a; Richmond et al., in press); *boulder ridges and ramparts* (Nott, 1997; Scheffers, 2004; Morton et al., 2008; Etienne and Paris, 2010); and *conglomerates* with marine bioclasts, attached to slopes (e.g. Moore and Moore, 1984; Shiki and Yamazaki, 1996; Felton, 2002; McMurtry et al., 2004; Pérez Torrado et al., 2006).

The use of coastal boulder accumulations for identifying past high-energy events has been extensively debated over the last decade, and their interpretation remains controversial (e.g. Scheffers et al., 2009; 2010; Goff et al., 2010a; Hall et al., 2010; Switzer and Burston, 2010). The presence of large boulders inland from rocky coasts could be a useful indicator for understanding the extent of the impact of past marine floods (Pignatelli et al., 2009), but identifying the specific cause of the marine flood (e.g. storm vs tsunami) remains debateable, unless convincing comparisons with modern analogues in the same or similar setting can be made. Studies of modern tsunami deposits can, at least qualitatively, relate the characteristics of tsunamis to their deposits (Jaffe and Gelfenbaum, 2007). Therefore, modern event investigations can provide benchmarks for numerical models, which in turn enable us to evaluate the likelihood of different emplacement mechanisms for palaeo-deposits of unknown origin. Studies of modern tsunamis prior to 2004 mainly focused on fine sediments deposited inland (e.g. Sato et al., 1995; Dawson et al., 1996; Minoura et al., 1997; Gelfenbaum and Jaffe, 2003) and very few contributions described coarse-grained deposits. While Shi et al. (1995) reported that hundreds of boulders were deposited as far as 200 m inland by the 12 December 1992 tsunami in Flores (Indonesia), no quantitative data were provided.

The aim of this paper is to evaluate what can be learned from boulders unequivocally deposited by two recent and well-documented tsunamis, the 2004 Indian Ocean (2004 IOT) and the 2009 South Pacific (2009 SPT) events. Three sites were investigated and documented: (1) Lhok Nga Bay, 10 km west of Banda Aceh (northwestern Sumatra, Indonesia), (2) Pakarang Cape near Khao Lak (western coast of Thailand), and (3) Satitoa (eastern coast of Upolu, Independent State of Samoa) (Figs. 1 and 2).

1.1. Tsunami background

The 2004 IOT was triggered by a Mw 9.15 earthquake at 0:58:53 GMT (Meltzner et al., 2006; Chlieh et al., 2007) that generated a 12 to 30 m slip on the plate interface (Ammon et al., 2005; Subarya et al., 2006; Koshimura et al., 2008. This was one of the largest tsunamis in recorded history, with 30 m high waves and runup locally reaching 51 m a.s.l. at Lhok Nga (Lavigne et al., 2009). Tsunami wave heights ranged between 15 and 30 m along the NW Sumatran coast, up to 13 m in Thailand, 11 m in Sri Lanka and 7 m in Eastern India (Choi et al., 2006). Flow velocities of 3 to 13 m s^{-1} were inferred from video analysis and eyewitness accounts in Sumatra (Fritz et al., 2006; Lavigne et al., 2009). Both runup and backwash produced extensive erosion, sediment transport and deposition up to 5 km inland in Sumatra (Paris et al., 2007), 1.5 km in Thailand (Hori et al., 2007), and 0.5 km in India and Sri Lanka (Bahlburg and Weiss, 2006; Morton et al., 2008). The erosional imprints of the tsunami extended 500 m inland from the shoreline and over 2 km up river channels in Sumatra (Umitsu et al., 2007; Paris et al., 2009). Boulders moved by the 2004 IOT were studied in Sumatra by Razzhigaeva et al. (2006) and Paris et al. (2009, 2010), and in Thailand by Goto et al. (2007), Kelletat et al. (2007) and Feldens et al. (2009).

The 2009 SPT was generated by two near-simultaneous earthquakes at the northern end of the Tonga Trench (Beavan et al., 2010; Lay et al., 2010), approximately 190 km south of Upolu (15,509°S, 172,034°W), Samoa (Lamarche et al., 2010). A M_W 8.1 normal faulting event on the outer trench-slope was followed within minutes by a M_W 8.0 subduction interface thrust event (Beavan et al., 2010; Lay et al.

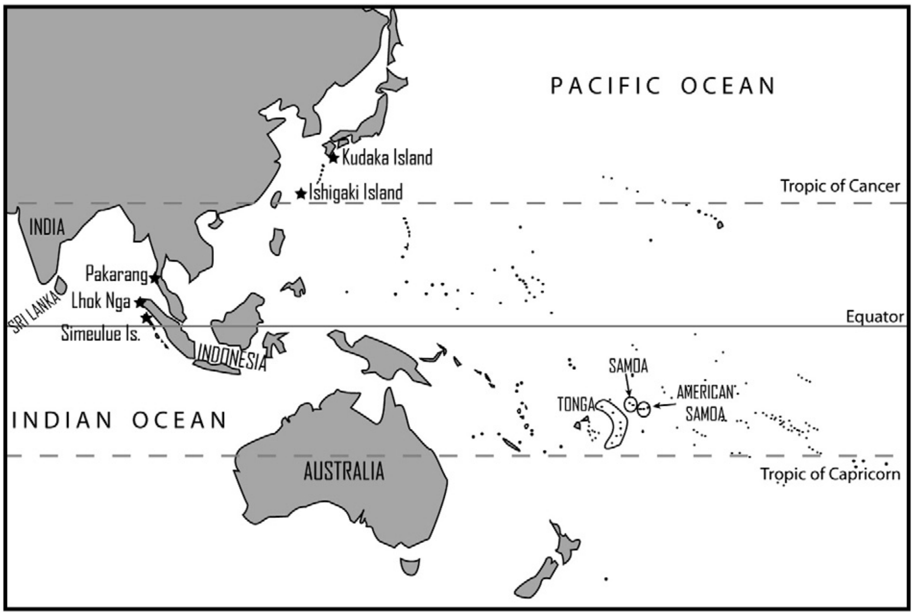

Fig. 1. Location map of key sites mentioned in the text (Samoa = Independent State of Samoa).

Author's personal copy

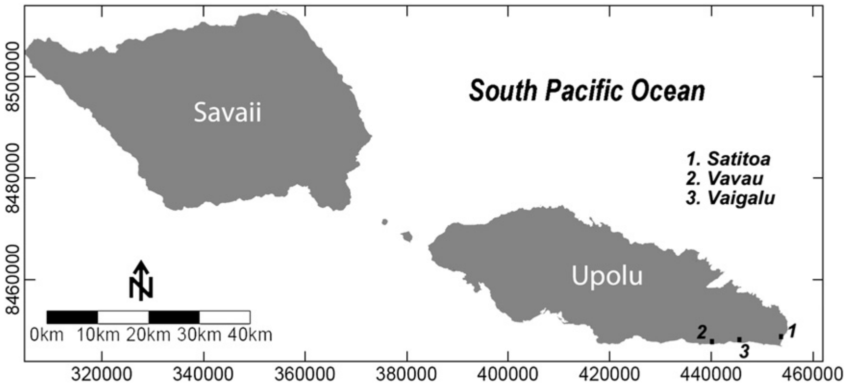

Fig. 2. Location map of Samoa showing key sites mentioned in the text.

2010). At the northern end of the Tonga Trench the Pacific Plate is subducting beneath the Australian Plate at extremely fast rates of up to 250 mm yr^{-1} but almost all of this convergence was previously thought to occur aseismically (Bevis et al., 1995; Ruellan and Lagabrielle, 2005). The earthquake doublet of 29 September 2009 showed that at least some plate convergence along this subduction margin is accommodated by co-seismic slip. The 2009 SPT impacted in Samoa, American Samoa, Tonga, Wallis and Futuna, and numerous locations in the central south Pacific. In Samoa, the tsunami consisted of two to three waves, with the second wave reported as the largest (Dominey-Howes and Thaman, 2009). Modelling of the tsunami suggests that arrival times of the first wave after the earthquake should have been 10 to 12 min on Upolu and Savaii Islands. Maximum flow depths of around 8 m occurred at Vaigalu and Vavau and 6.2 m at Satitoa (Fig. 2), while the maximum runup of 14.3 m was measured at Vaigalu (Dominey-Howes and Thaman, 2009). In the Wallis and Futuna archipelago the tsunami reached 4.5 m asl and inundated up to 85 m inland (Lamarche et al., 2010). Other effects are discussed in papers presented in this issue (e.g. Clark et al., this issue; Richmond et al., 2011).

2. Where do tsunami boulders come from?

Identification of the source is an important issue in the study of boulder deposits. The lithology, surface morphology, texture and structure of boulders may provide evidence of their geographic origin and physiographic setting before they were transported inland (i.e. pre-transport environment: subaerial, submerged, or joint-bounded). The pre-transport environment can be assessed using various environmental markers on boulders, such as the boulder shape. For example, similarities between coral boulders and rocks found around the spurs and grooves of reefs help identify the pre-transport environment (e.g. Onda, 1999). Different forms of weathering are also valuable environmental markers. For example, karstic pools on limestone boulders suggest weathering in the mid-supralittoral zone (Scicchitano et al., 2007), and may also be used to assess exposure and thus the time since deposition. Attempting to decipher both of these markers requires detailed observations about the position of the karstic pool, floral and faunal communities associated with it and exposed fracture surfaces (Scicchitano et al., 2007). Biological encrustations and characterisation of coral species can be used to identify the littoral zone from which the boulders were entrained (e.g. Goff et al., 2006b; Scicchitano et al., 2007). For example, in Thailand, Goto et al. (2007) studied more than 1000 boulders left by the 2004 IOT on a tidal flat west of Pakarang Cape (Khao Lak). All boulders came from coral colonies only found at shallow depths of less than 5–10 m. Well-preserved *Balanus* barnacle shells were found attached to the flat surfaces of the boulders and these were used to determine the original upper side of each boulder. Finally, boulder lithology, if unusual, can often be associated with a particular area, thus identifying the source location (e.g. beachrock in Paris et al., 2009).

These different pre-transport environments determine the energy required to move the boulders. Nott (2003) distinguishes three boulder types from their potential pre-transport environment; subaerial, submerged and megaclasts derived from joint bounded blocks on shore platforms. Boulder transport requires large drag-and-lift forces particularly if megaclasts are broken off from rocky platforms, terraces or reefs. The withdrawal of the sea (trough) prior to the arrival of the first wave (crest) of the 2004 IOT (according to eyewitness accounts the sea withdrew ~1 km at Lhok Nga — Lavigne et al., 2009), caused air to be trapped in the joints and fractures of the shore platform. Air is then suddenly compressed as the positive wave arrives and, as the wave subsequently recedes, the air expands with explosive force to exert an outward stress on the bedrock (Sunamura, 1992). This process of wedge action could generate sufficient force to detach individual boulders from the shore platform.

The 2004 IOT moved a large quantity of sediment and debris at sites all along the western coast of Sumatra, both onshore and offshore (Umitsu et al., 2007; Paris et al., 2009; 2010). Eyewitness accounts in Sumatra recall waves already black with sediment before breaking inland (Lavigne et al., 2009). The simulation of threshold shear velocities estimated by Paris et al. (2010) confirmed that most of the sediment deposited inland – from fine sands to coral boulders – probably came from offshore. Paris et al. (2009) estimated that the volume of beach eroded by the tsunami in Lhok Nga (ca. 0.15×10^6 m^3 over 9.2 km of coast) was less than 10% of the sediments deposited inland (ca. 1.5×10^6 m^3). Although the volume of sediments left inland by the tsunami was mainly represented by extensive sheets of sand-size sediments, coarse soil clasts, concrete and rocks were also deposited onshore.

Paris et al. (2009) measured 220 boulders in the Lhok Nga area, most of them with long-axis lengths between 0.7 and 1.5 m and volumes between 0.1 and 0.9 m^3. Four boulder sources were identified (Fig. 3, Table 1). The first was located south of the main river mouth, where limestone boulders up to 7.7 tons were lifted from a seawall and deposited up to 200 m inland (Figs. 3B and 4). The total number of boulders transported from this site was probably over 1000, and all were found along a 250 m strip parallel to the coast between the seawall and the main road. The second source was south of Lhok Nga Harbour, where tabular megaslabs up to 85 tons were dislodged from the tidal flat, overturned and deposited a few metres inland (Figs. 3C and 5). The source area for the megaslabs is visible when the sea is calm and indicates that these blocks were joint-bounded prior to the tsunami. In Lampuuk and Lhok Nga, 80 coral boulders up to 11.4 tons from a third source were deposited up to 900 m inland (Fig. 6). A side-scan sonar survey in Lhok Nga Harbour revealed that all rocky outcrops up to 25 m deep (old reefs, isolated knolls) were affected by the tsunami, but that the contemporary fringing reefs in Lampuuk and Lhok Nga were not the main sources of the boulders (Paris et al., 2010). Beachrock near the Lhok Nga River mouth acted as a fourth source and provided boulders up to 600 kg that were deposited up to 335 m inland, most of them being concentrated between 80 and 110 m from the shore.

Author's personal copy

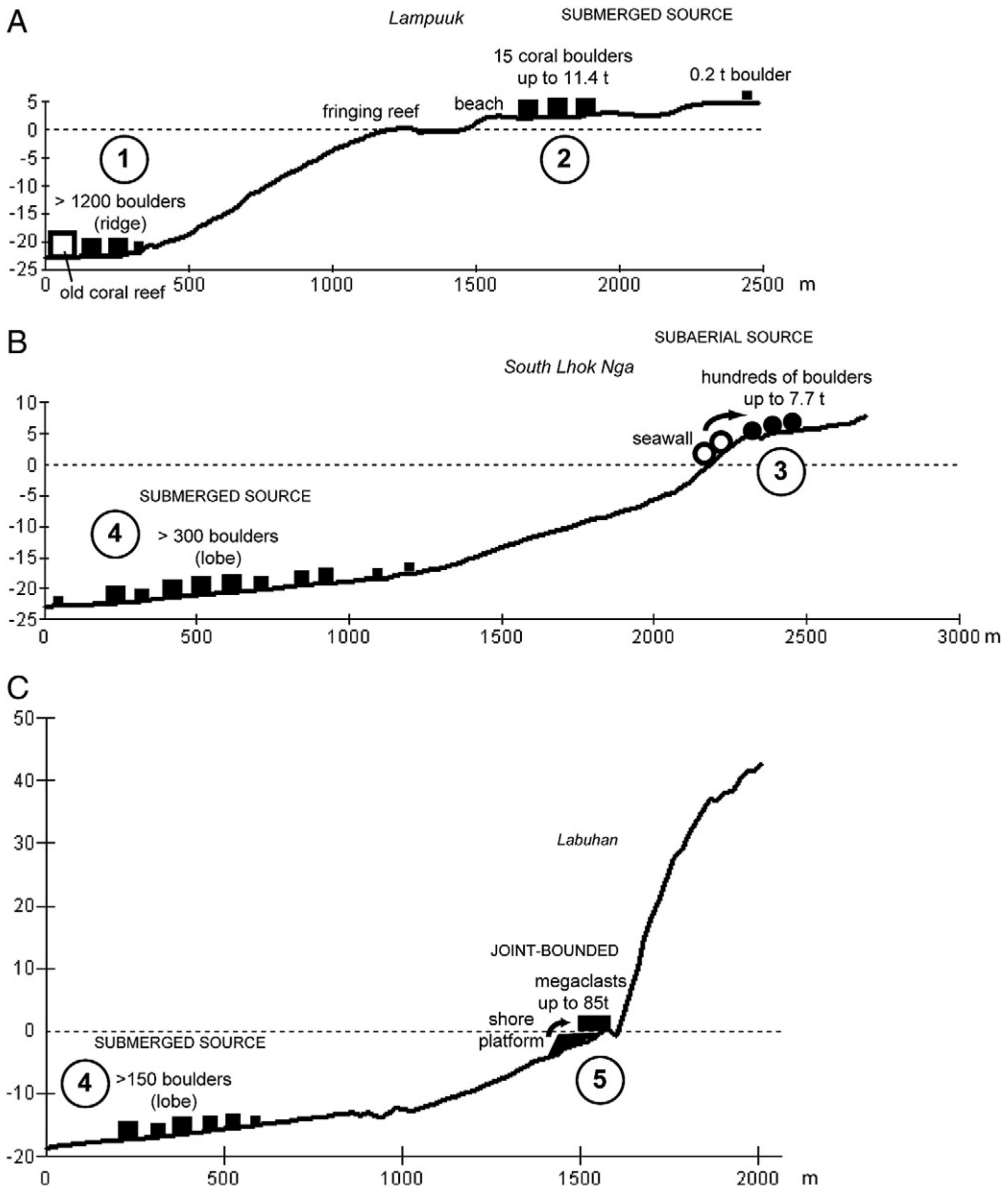

Fig. 3. Longitudinal profiles showing different pre-transport environments and spatial distribution of boulders deposited by the 2004 tsunami in Lhok Nga (northwest Sumatra). Offshore boulders were identified by side-scan sonar survey (Paris et al., 2010). A) Lampuuk area. (1) coral boulders detached from old coral reefs at −25 m bsl, moved during tsunami runup; (2) few of them being transported inland). The other boulders are reworked offshore by the powerful backwash and thus deposited as ridges on the landward face of the old reefs. B) south of the Lhok Nga River, (3) hundreds of calcareous boulders up to 7.7 t were detached from a seawall and transported inland as far as 200 m (reworked by backwash?). C) off South Lhok Nga, the distribution of boulders describes a large lobe (4) that was interpreted by Paris et al. (2010) as a density flow during the tsunami backwash. In Labuhan area, mega-slabs of conglomerate (5) up to 85 t dislodged from the shore platform and deposited close to the shoreline in overturned position (joint bounded scenario).

The 2009 SPT also carried a large quantity of sediment and debris and eyewitness accounts described the tsunami as black or dark (Dominey-Howes and Thaman, 2009). Extensive sand sheets and boulder deposits were laid down inland (see Richmond et al., 2011; Jaffe et al., 2011). Boulders had different sources and lithology: basalt from coastal engineering structures (Satitoa, Fig. 7), basaltic pieces from volcanic cliffs (Savaii, Fig. 8) and individual coral colonies from shallow lagoons and reef flats.

Table 1
Boulder sources and main characteristics of deposits near Lhok Nga, Sumatra.

Source	Lithology	N boulders	Max volume	Max mass
Seawall	Limestone boulders	>1000	3.2 m^3	7.7 t
Rocky platform	Megaslabs	>10	60 m^3	85 t
Reefs	Coral boulders	>80	10.5 m^3	11.4 t
Beachrock	Beachrock boulders	>15	1.4 m^3	2.5 t

3. Spatial distribution of boulders

In tsunami deposits, boulder accumulations in whatever form never appear to be transported great distances inland and are therefore normally in a close association with their source location. In Sumatra, the mean transport distance of the 220 boulders mapped by Paris et al. (2009) after the 2004 IOT was 178 m, with only 3% transported more than 450 m from the shore (Fig. 9). In Lhok Nga, the longshore extent of boulders dispersed from the seawall corresponded to the length of the source wall, and any landward transport was minor. Razzhigaeva et al. (2006) studied 2004 IOT deposits and reported numerous coral boulders along the coasts of Simeulue Island, noting in particular large overturned boulders 400 m from the shoreline at Langi where tsunami runup reached 9 m. Goff et al. (2006b) reported boulders up to 7.9 m a.s.l. and 14.8 m inland along the southern coast of Sri Lanka. Conversely, at Pakarang Cape (Thailand) no boulders were found on land, indicating that the hydraulic forces of the tsunami wave

Author's personal copy

Fig. 4. Seawall impacted by the 2004 tsunami in Lhok Nga (northwest Sumatra), source of an 82,000 m² field of calcareous boulders up to 7.7 t.

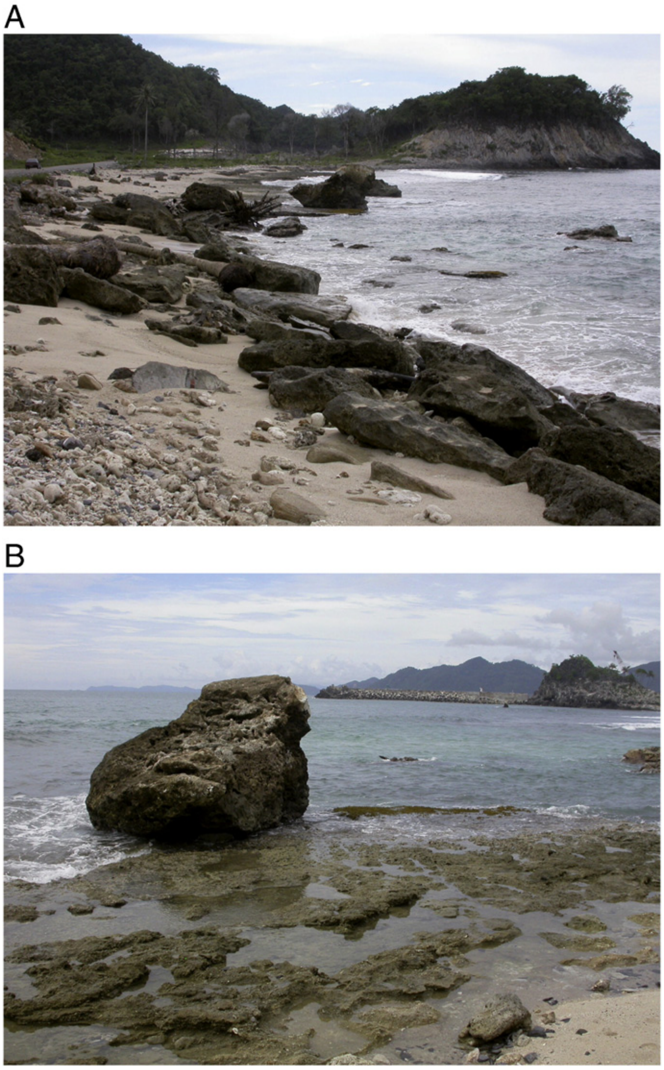

Fig. 5. A) general view of mega-blocks deposited on land by the 2004 tsunami south of Lhok Nga Harbour (northwest Sumatra, Tsunarisk project); B) the largest boulder of 85 t.

rapidly dissipated across the shore platform (Goto et al., 2007). All boulders were found within the intertidal zone, and their deposition along three arcuate lines has been attributed to long-lasting oscillatory flows leading to clast grading (Goto et al., 2007).

In Satitoa, Samoa, riprap boulders were moved landward and deposited less than 162 m from the revetment. This distance was not measured shore normal, but conformed to the mean tsunami flow direction deduced from flow indicators in the field. The mean transport distance of the 162 boulders from the revetment was 81 m, with 5% of the boulders transported more than 140 m from the shoreline (Fig. 10). A concentration of boulders (49% of boulders) can be observed 80–120 m from the seawall in the mean tsunami flow direction.

In Lhok Nga, Sumatra, side-scan sonar surveys revealed that the amount of boulders transported from offshore and deposited on land represented only 7% of the total number of boulders moved during the 2004 IOT (Paris et al., 2010). Almost 8000 objects were identified offshore here of which 2894 pieces of anthropogenic debris, 1760 boulders, 286 tree trunks and 1119 fragments of undifferentiated small debris were most probably moved by the tsunami. The spatial distribution of the boulders is most likely controlled by submarine morphology, such as fringing reefs and rocky platforms. Feldens et al. (2009) also observed boulders in channels off Cape Pakarang (Thailand) and suggested that they were transported by tsunami backwash.

4. Types of boulder accumulations

4.1. Mega-blocks on coastal platforms

The largest mega-block attributed to a tsunami is up to 15 m in length, with a volume of 1500 m³ and a weight of 2000 tons (Frohlich et al., 2009). Bourrouilh-Le Jan and Talandier (1985) have suggested that mega-blocks up to 1000 m³ and about 1500–2000 t found in Rangiroa, French Polynesia, might have a tsunami origin, but as the source event is not clearly identified, they did not preclude a cyclonic origin (Talandier and Bourrouilh-Le Jan, 1987). Hyvernaud (2009) has recently challenged the tsunami origin proposed by Talandier and Bourrouilh-Le Jan (1987) by tracking satellite evidence of contemporaneous geomorphic impacts on several atolls in the Tuamotu Archipelago. Preferential boulder distribution around atolls and the relative alignment of impacts, coupled with ^{14}C dating could favour an 18th century cyclone event dated to around 1715 AD ± 60 yr (Hyvernaud, 2009).

Author's personal copy

Fig. 6. Coral boulders deposited by the 2004 tsunami in Lhok Nga (northwest Sumatra), (A) at the nearshore, and (B) 480 m inland (750 m from the reef), 11.5 t boulder.

At Inoda, on the Miyako-Yaeyama Islands, Japan, the 1771 Meiwa tsunami transported limestone boulders up to 600 m^3 as much as 200 m inland (Goto et al., 2010b). Tsunamis generated by the 1883 Krakatau eruption moved many coral boulders along the coasts of the Sunda Strait. The largest had an estimated weight of 450–500 t (Verbeek, 1886). Boulders deposited by the 2004 IOT in Sumatra were not as large, with a maximum weight of 85 t on the beach and 11.5 t at 750 m distance from the reef, even though the mean nearshore wave heights were greater than those in the Krakatau tsunami (20–30 m in Lhok Nga, 15 m in Anyer). This comparison confirms that the maximum boulder weight carried by tsunami waves appears to be influenced by the pre-transport setting at the boulder source and that size alone might not accurately reflect the tsunami's flow characteristics.

4.2. Fields of scattered boulders and boulder clusters

Most of the accumulations from the 2004 IOT are represented by fields of scattered boulders displaying local arrangements such as imbricate clusters in south Lhok Nga (Paris et al., 2009) and boulder trains along preferential lines of deposition in Pakarang Cape (Goto et al., 2007). Many similar enigmatic boulder fields previously described over the world have also been attributed to tsunamis (e.g. Mastronuzzi and Sansò, 2000, 2004; Whelan and Kelletat, 2005; Scheffers and Scheffers, 2007; Scicchitano et al., 2007; Maouche et al., 2009). Nevertheless, it is often difficult to exclude a storm or cyclone origin because these types of boulder accumulations are also common on rocky coasts not affected by tsunamis (e.g. Suanez et al., 2009). Goto et al. (2010a) studied boulder distributions in two groups of Japanese islands, one being affected by storms and tsunamis, the other by storms only. This comparative approach provides valuable data for determining the sedimentary features of tsunami boulder fields and the characteristics of storm wave boulders.

4.3. Boulder beaches, ridges and ramparts

As far as we know, the 2004 IOT and 2009 SPT did not form boulder beaches. This type of accumulation is found exclusively in the high-energy environments of rocky coasts dominated by storm conditions (e.g. Northern Ireland: McKenna, 1990; Iceland: Etienne, 2007; Etienne and Paris, 2010) or affected by swells generated by low pressure systems (e.g. Smith et al., 2010). A fundamental distinction between storms and tsunamis could be the ability of storms to form boulder ridges and boulder beaches. Indeed, the organisation of coarse clasts into ridges requires repeated reworking by many waves rather than only the impact of a few waves, as occurs during a tsunami (Williams and Hall, 2004). There are no published accounts of extensive boulder ridge formation by a tsunami in any case studies of recent events. Along the western coast of Sumatra, cobble-to-pebble ridges were deposited on rocky coasts and behind fringing reefs during the weeks and months that followed the 2004 IOT, thus contributing to beach recovery, but they were not observed three weeks after the tsunami (Paris et al., 2009). In Pulau Pangan Island (Simeulue), Razzhigaeva et al. (2006) observed a small rampart up to 1.4 m high composed of coral fragments near the shoreline and concluded that it was formed at the final stage of the tsunami during frequent low-amplitude sea level fluctuations. Distinguishing between the two different processes appears to be subtle, but not insurmountable (Goff et al., 2010b).

The extensive cobble-to-boulder ridges and ramparts described by Scheffers (2004) in the Leeward Netherlands Antilles are the only ridge-like features attributed to tsunamis so far studied. More recently however, Spiske et al. (2008) did accurate calculations of the porosity of the boulder clasts from the ridges and found them to be up to 5.6 times lighter than reported in previously published data, thus resulting in lower minimum wave heights required for their transport. Based on revised transport calculations combined with the boulder ridges occurring predominantly along the windward coasts and the high frequency of tropical storms and hurricanes in the region, Spiske et al. (2008) stated that a hurricane origin was more likely for the ridges.

4.4. Cliff-top boulders

Cliff-top deposits up to cobble-boulder in size have been reported from numerous locations but especially in the North Atlantic (Williams and Hall, 2004; Hall et al., 2006; Suanez et al., 2009; Etienne and Paris, 2010) and Hawaii (Goff et al., 2006b; Richmond et al., in press). Unfortunately, little information is available for coastal

Author's personal copy

A

B

Fig. 7. Riprap revetment as a boulder source in Satitoa, Samoa. (A) aerial view of the demolished revetment the day after the tsunami (picture: NZAF, 30/09/09); (B) view of the riprap revetment partially reconstructed (S. Etienne, 20/10/09).

Fig. 8. Boulders detached from the cliff-edge by tsunami waves. Savaii, Samoa. Picture: S. Etienne, 21-10-2009. Dotted lines show fresh scars on the reef edge. White arrow indicates rectangular boulder.

cliffs impacted by the 2004 IOT and 2009 SPT. In Savaii, Samoa, only small boulders uprooted from the basaltic cliff edge are indisputably of tsunami origin (Fig. 8).

4.5. Marine conglomerates

In the southern part of Lhok Nga Bay, Paris et al. (2010) interpreted a lobe-like distribution of boulders as being the result of a subaqueous sedimentary density flow (Mulder and Alexander, 2001) that formed during 2004 IOT backwash. This density flow was captured in a Spot-2 image acquired 3 h after the tsunami. The lobe-like distribution has a higher density and larger boulders at the seaward edges. Such a density flow in the southern part of the bay can be explained by interactions between the tsunami wave and nearshore topography. Where the tsunami inundation was hindered by steep slopes, debris and sediments could not be deposited far inland, and were re-transported offshore by the final backwash. The outflow remained saturated in debris, and this dense sediment-water mixture may have behaved in a similar fashion to a Bingham fluid dominated by shearing and frictional debris interactions (Paris et al., 2010).

Deposits interpreted as density flows during tsunamis have been described in the literature but were never observed prior to 2004. Debris-flow conglomerates with shear carpet indicate very dense and

Author's personal copy

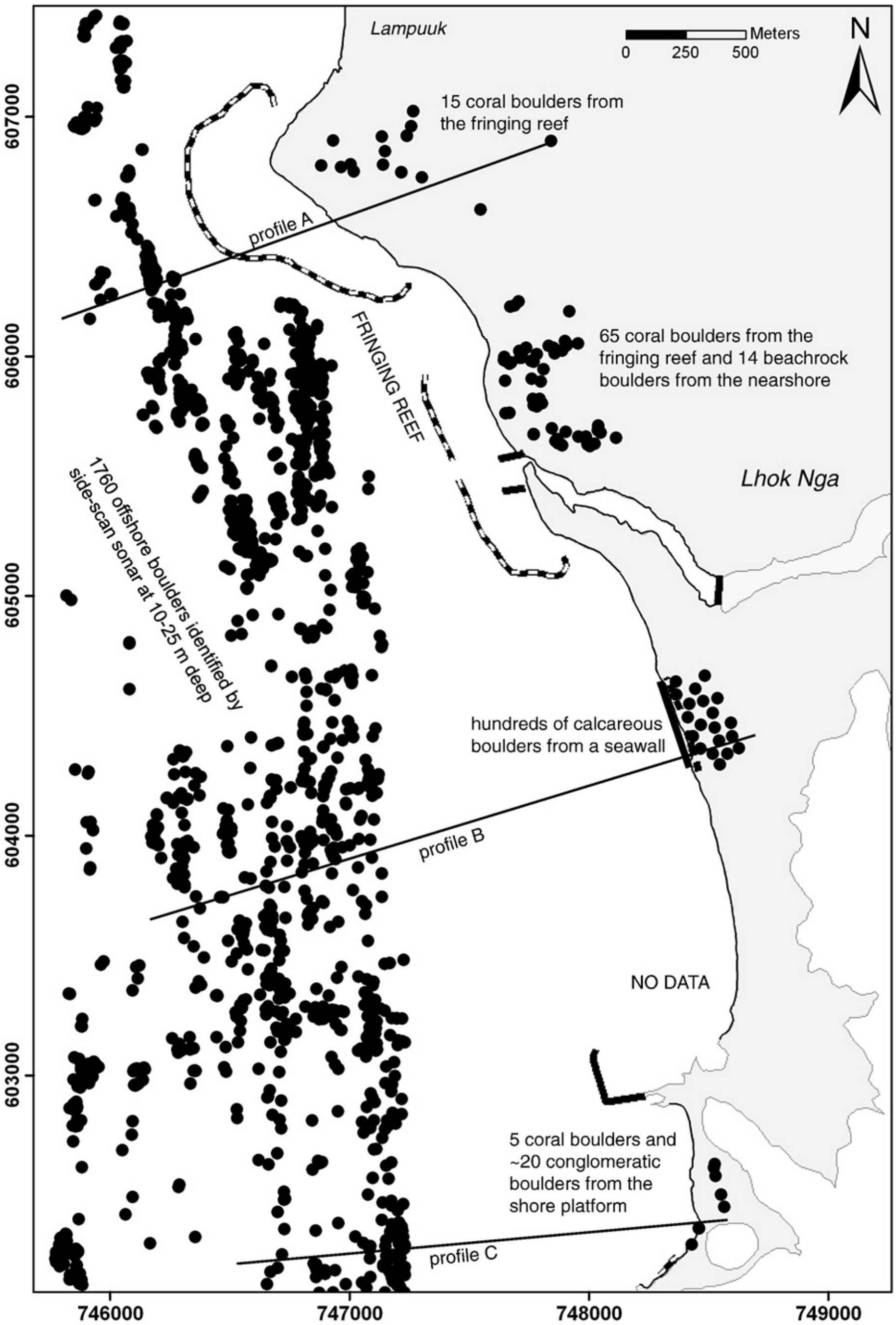

Fig. 9. Map of boulders transported and deposited by the 2004 tsunami in Lhok Nga Bay, northwest Sumatra, (modified after Paris et al., 2009, 2010). Offshore boulders were identified by side-scan sonar survey.

highly sheared fluid conditions. Such flows possibly behaving with Bingham characteristics have been described from Chile (Le Roux et al., 2004; Le Roux and Vargas, 2005) and Japan (Shiki and Yamazaki, 1996). Debris flow deposits on the western coast of Gran Canaria (Paris et al., 2004) and coarse breccias on the steep slopes of Stromboli Island (Tanner and Calvari, 2004) have also been interpreted as the result of tsunami backwash. Cantalamessa and Di Celma (2005) described a boulder-bearing breccia in northern Chile and inferred that it had been laid down by subaqueous density flow during tsunami outflow. However, Bahlburg and Weiss (2006) have contested this and interpret the breccia as a debris-flow deposit connected to the formation of a graben rather than a tsunami. The study of submarine tsunami deposits is still in its infancy and as such researchers need to work diligently to develop their process interpretations.

5. Transport distance vs boulder size and weight

Goto et al. (2010c) infer that there is no simple relationship between tsunami magnitude and the weights and numbers of boulders it transports. As the duration of a tsunami wave force acting on the boulder is considerably longer than that of a storm wave, the difference in transport distance of boulders by a storm or tsunami might be a useful way to differentiate between them (Goto et al., 2010b), but differences in wave energy attenuation have to be considered too.

A rough estimation of the transport energy for boulder movement is given by the “transport figure” (Scheffers and Kelletat, 2003), which is simply the result of multiplying the boulder weight, distance from the shoreline and height above sea level. Transport figures have been proposed to decipher the origin of boulder deposits. The transport

Author's personal copy

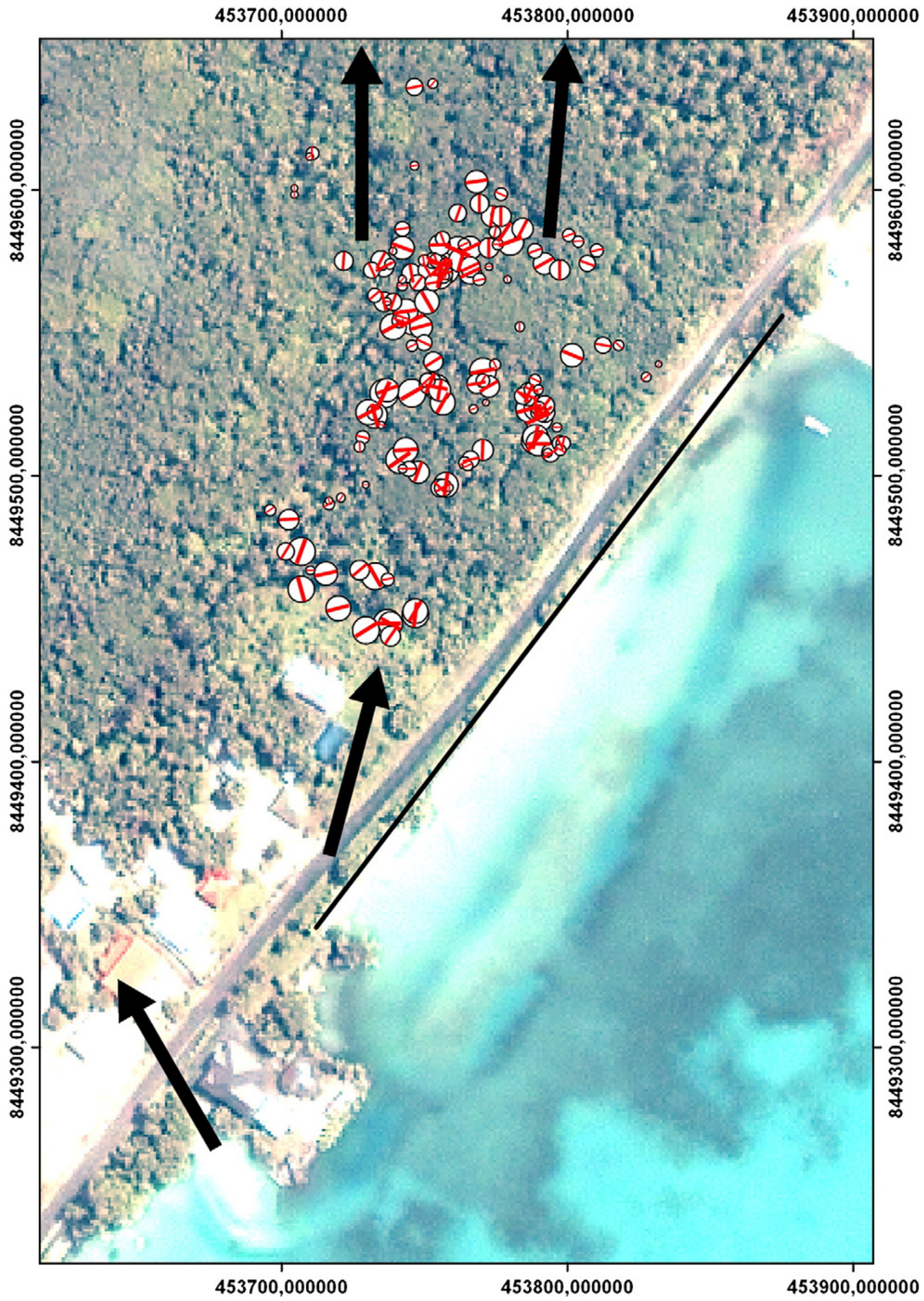

Fig. 10. Map of boulders transported and deposited by the 2009 tsunami in Satitoa, east Upolu, Samoa. Circle proportional to boulder volume (max: 1 m^3). Red bar indicates A-axis orientation, black arrows indicate mean flow direction and the black line signals boulder source.

figures for the 2004 IOT in Lhok Nga range from 8000 to 45,000 for the boulders from the coral reef, less than 13,000 for megaclasts from the shore platform and less than 10,000 for limestone boulders from the seawall (Paris et al., 2009). Transport figures exceeding 70,000 and even 1,000,000 were calculated for coastal boulders in the Netherlands Antilles and in Australia (Scheffers and Kelletat, 2003). For storm boulder deposits in Iceland, the transport figure is almost always under 5000 (Etienne and Paris, 2010).

In Satitoa, nearly all boulders from the rock armour were transported inland by the 2009 tsunami, meaning that the transport capacity of the waves was higher than can be deduced from the measured boulders themselves. No boulder was greater than 1 m^3, but the maximum volume of transported boulders was limited by source availability (i.e. the rock armour). In Pakarang Cape, Goto et al. (2007) measured 467 boulders, with the largest being 14 m^3 with a weight of about 22.7 t. Kelletat et al. (2007) noted two granite boulders of 4 t and 10 t moved by the 2004 tsunami at Khao Lak, coral boulders up to 10 t in Nai Harn Noi, and up to 40 t at Phi Phi Don tombolo. In Sumatra, hundreds of boulders were moved offshore but not deposited onshore. The largest coral boulders identified offshore measured 14.8×6.9 m, compared to $3.5\times2.5\times1.8$ m onshore (11 t). 85 t slabs south of Lhok Nga were overturned on the tidal flat and transported only a few metres. Thresholds of transport capacity can be inferred from the size and weight of these emerged boulders and Paris et al. (2010) estimated the movable grain sizes based upon simulated current velocities of the tsunami waves (e.g. Maeno and Imamura, 2007; Noda et al., 2007). In these cases, boulder mass is a more useful tool for determining the threshold transport capacity since boulder density ranges from 1 to 3 (a 1 m^3 basaltic boulder having approximately the same mass as a 2.5 m^3 coral boulder).

Author's personal copy

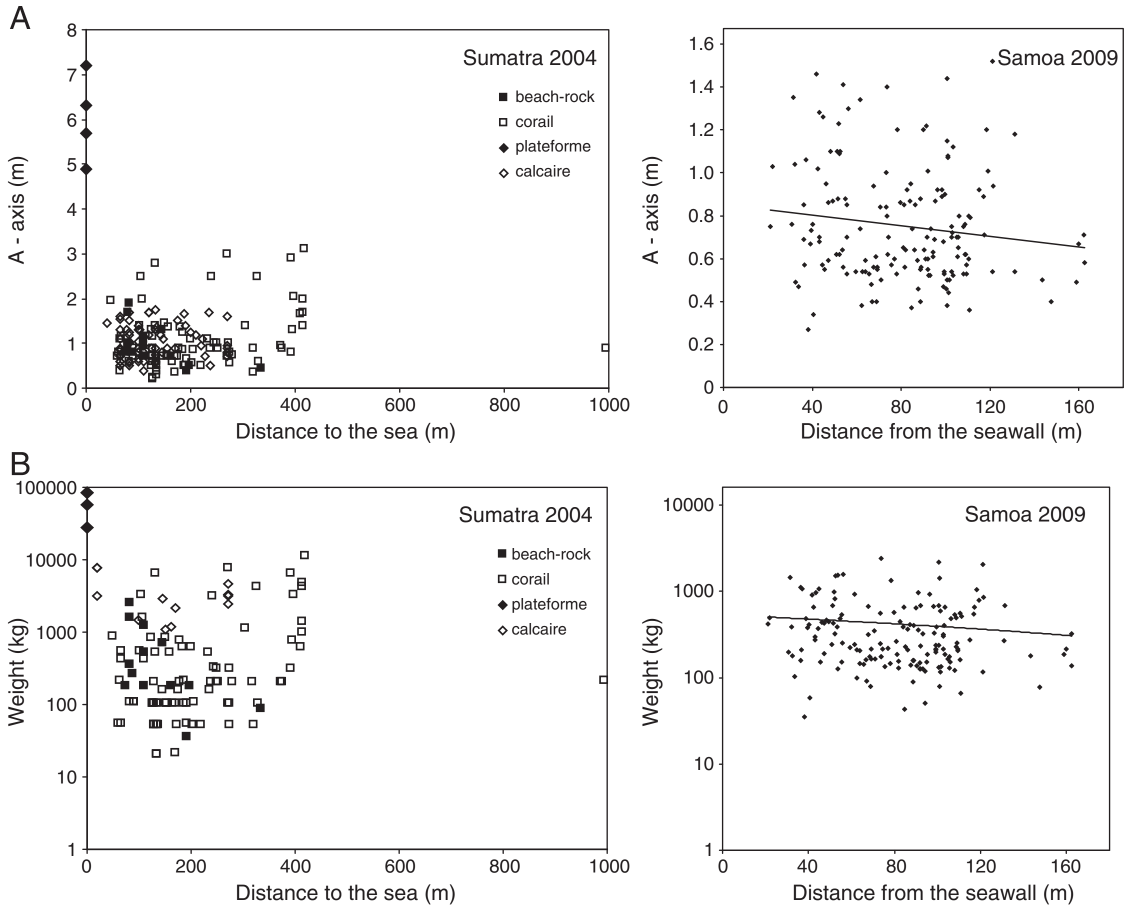

Fig. 11. Relationship between boulder length (A) and weight (B) with distance from the source in Lhok Nga, Sumatra, and Satitoa, Samoa.

Nevertheless, there is no clear relationship at either Lhok Nga or Pakarang Cape between the size and weight of the coral boulders and their location inland (Paris et al., 2009, Goto et al., 2007). Only the beachrock clasts in Lhok Nga displayed a landward fining trend (Fig. 11). Interestingly, these beachrock clasts (density = 1.79 $g\,cm^{-3}$) were transported almost the same distance as denser calcareous clasts from the seawall (2.4 $g\,cm^{-3}$). There is no landward fining of the basaltic boulders detached from the seawall in Satitoa (Samoa) either. In Lhok Nga, the weight of offshore boulders cannot be estimated, but boulder-size trends along lateral and longitudinal transects were tested by Paris et al. (2010). These authors found no clear boulder-size gradient, except in the southern part of the Lhok Nga Bay, where a subaqueous sedimentary density flow resulted in the seaward coarsening of the boulders (see Section 4). Elsewhere, the backwash influence on boulder distribution was difficult to determine. Numerical modelling of the tsunami backwash however, suggests that flows were powerful enough to rearrange the distribution of small-size boulders both onshore and offshore (Loevenbruck et al., 2007).

The comparison between the impacts of the 2009 SPT and 2004 IOT on two boulder rock armours shows similar characteristics, such as limited extent of landward transport and the absence of landward fining. The latter might be explained by inter-clast interaction/collision; when a tsunami wave travels over a rocky platform it gradually incorporates boulder-sized clasts when available. In a rip-rap revetment context, all boulders are available (i.e. not cemented or attached to the ground), and can be mobilised over a short time span and distance, due to the homogeneity of boulder size, if the flow velocity is high enough for their entrainment. It is probable that all boulders start moving together, which favours collision and interaction between them. The same discrepancy of massive rock piece transport and deposition has been observed in the Akita Prefecture of Japan where 4 t concrete tetrapods ("boulders" with similar shape and weight) were washed inland by 1983 tsunami waves (see Fig. 1 in Yeh, 1991). Conversely, storm wave boulder fields show an exponentially fining landward feature (Goto et al., 2009; Etienne and Paris, 2010; Goto et al., 2010b). This characteristic might be explained by the attenuation of storm wave energy due to wave breaking and bottom friction that limits the capacity of storm waves to transport large clasts a great distance inland (Buckley et al., in press).

As boulders from riprap revetment (rock armour) have been artificially shaped (i.e. for engineering purposes), the flatness index ($F_b = (A + B)/2C$, cf. Cailleux and Tricart, 1959) has no genetic significance, but it can be used to estimate the interaction between shape and transport. An F_b close to 1 means that the boulder is rounded, ellipsoidal or cubic, while higher values mean that the boulder is elongate (Table 2). There is however, no strong relationship between transport distance and flatness index, neither from Sumatra nor the Samoa boulders (Fig. 12). However, basaltic boulders that were transported the farthest inland in Satitoa have F_b values under 2.2, whereas boulders with F_b value over 4 are found less than 80 m

Table 2
Flatness index for Satitoa boulders.

Distance from the revetment (m)	Mean flatness index
21–50	2.04
51–80	1.98
81–110	1.88
111–140	2.09
141–162	1.61

Author's personal copy

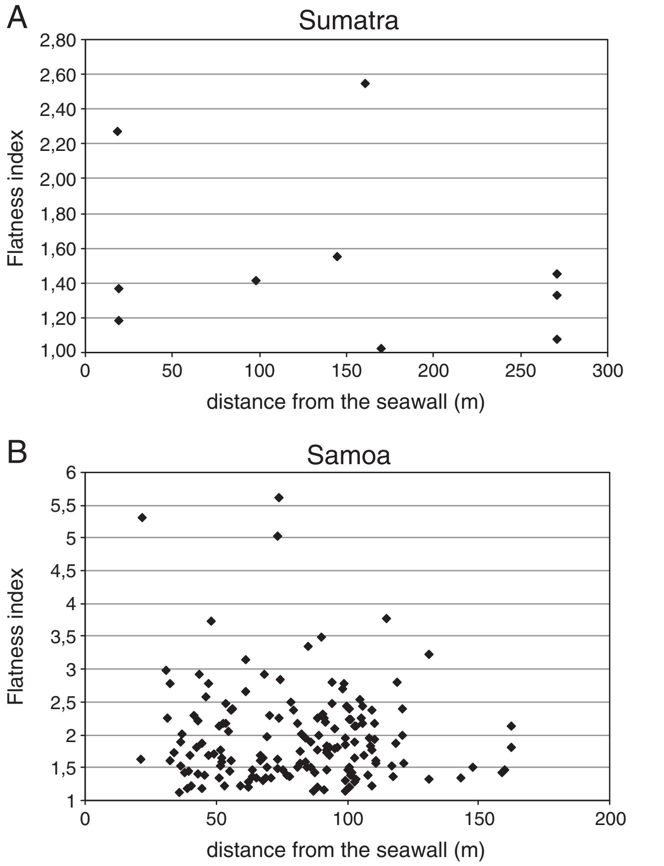

Fig. 12. Boulder flatness index versus distance from the source. (A) Lhok Nga, (B) Satitoa.

from the source (Fig. 12B). We suggest that this index be tested by other authors with their own data.

6. Are boulders indicative of flow direction?

In Pakarang Cape, the orientation of the long axes of boulders were variable due to the microtopography of the tidal flat, but an overall N-S orientation perpendicular to the flow direction was dominant (Goto et al., 2007). Interestingly, these orientations were not realigned by the

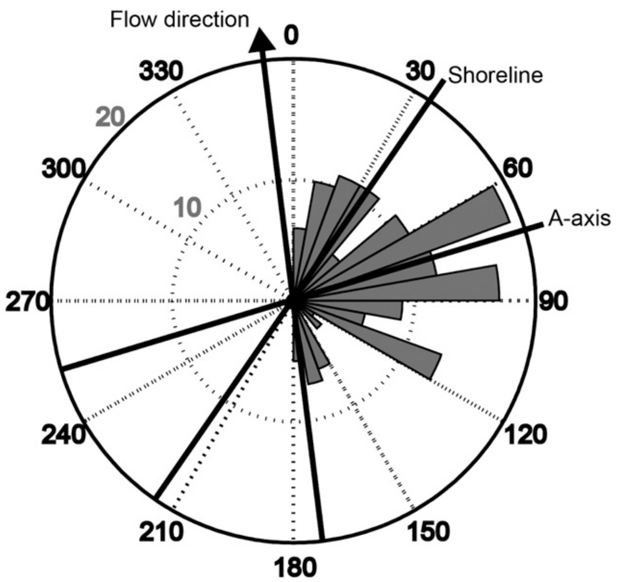

Fig. 13. A-axis orientation of transported boulders at Satitoa, Samoa in 10° sectors.

monsoonal storms that followed the 2004 IOT. At Lhok Nga, the large elongated boulders were also mostly imbricated with their long axis perpendicular to the direction of tsunami flow. Imbricate clusters also show similar trends in relation to the tsunami flow direction, thus supporting the interpretation that the largest boulders deposited inland were not reworked or removed by the backwash (Paris et al., 2009).

In Samoa, the A-axis orientation was recorded for 153 boulders (Fig. 13). 49% lie in the N045-104 class, with a 10° sector modal class at N057-066. The mean A-axis orientation (N073) is approximately perpendicular to the mean measured flow direction (N353; Fig. 12) and is within 45° of the shoreline orientation (~N035).

The distribution of the long and imbrication axes may help reconstruct the direction of a tsunami wave train and distinguish different flows (successive waves, backwash) although it should be noted that subsequent storms may be able to modify the position of some large boulders (Noormets et al., 2002; Felton and Crook, 2003). Clast-to-clast interactions and microtopography may also influence the final disposition of boulders, especially in terms of tilting (inclination of C-axis), but for Samoa and Sumatra most of the clasts were transported over gentle slopes such as shore platforms and coastal plains, without significant breaks in slope.

7. Transport modes

Boulders can be transported by sliding, rolling or saltation. In experiments conducted by Imamura et al. (2008), boulders are mainly seen to be transported by a bore through rolling or saltation rather than sliding. Experimental studies have shown the transport mode can vary with changes in the flow velocity, bottom friction, and shape and weight of the boulder (Goto and Imamura, 2007).

Goto et al. (2007) argued that the boulders left by the 2004 IOT in Pakarang Cape were transported by rolling or saltation rather than sliding. Boulders observed onshore in Lhok Nga were partially buried by sandy tsunami deposits, without any ejecta or impact features. The surface morphology and the structure of the largest *Porites* boulders showed that they were often in overturned positions (Paris et al., 2009). Nevertheless, the coincidence of different size modes, from boulders to fine sands suggests that all the material was not transported in suspension, but that there was a combination of bed load and suspended transport (Goff et al., 2006b; Paris et al., 2007, 2009). Nandasena et al. (in press) recently introduced a method to estimate the range of current velocity that satisfies the initial transport of a boulder in different modes (sliding, rolling and saltation), thus predicting the possible initial transport mode of a boulder with a given velocity. This method was applied to boulders deposited on land by the 2004 IOT in Lhok Nga, and it was inferred that beachrock boulders no larger than 2 m had been transported both by rolling and saltation. All coral boulders can easily be moved by the tsunami flow (assuming a density of 1.12) and calculations suggest that the dominant transport mode is saltation. Limestone boulders from the seawall have higher densities (2.4 g cm^{-3}) than corals (~1.2 g cm^{-3}) and thus require current velocities higher than 3–4 m s^{-1} to be transported by sliding or rolling, and higher than 11–12 m s^{-1} for saltation. Velocities estimated by numerical and mechanical models ranged between 3 and 8 m s^{-1} in this area (Paris et al., 2010). Conglomerate boulders exhibited only two possible modes in the histogram, as they were joint-bounded in their pre-transport setting and lifted from their initial position. Following the model, current velocities higher than 9–10 m s^{-1} are required to initiate their transport, and field velocities estimated by Paris et al. (2010) were lower than 13 m s^{-1}. Thus, the model correctly predicts what occurred — that these megaclasts could only be transported a few metres.

8. Are boulders indicative of flow velocity?

In the literature, boulder deposits have been used to infer minimum flow velocity and wave heights for past extreme wave events

Author's personal copy

Table 3
Tsunami flow velocities estimated after the characteristics of the largest boulders transported and deposited both offshore and inland, compared with flow velocities estimated after numerical modelling and eyewitness accounts. The range of distance from the shore is given for all boulders observed. Note that the distance from the shore indicated for offshore boulders is not representative of the tsunami inflow velocities (modified after Paris et al., 2010).

Boulder setting	Tsunami inflow velocity (m/s)		Distance from the shore (m)
	from numerical modelling and eyewitness accounts	from characteristics of boulders	
Coral boulders deposited inland	3–12	>3.7	48–995
Beachrock boulders deposited inland	3–9	>4.0	37–335
Calcareous boulders from seawall	3–8	>3.9	5–270
Joint-bounded megaclasts from tidal flat	3–7	>6.2	<5
Coral boulders identified offshore	8–13	>7.5	(up to 3000)

(e.g. Imamura et al., 2008). Flow velocity calculations are performed by balancing the fluid forces or moments with either the resistance force for sliding or the resistance moment for overturning. Paris et al. (2010) calculate the minimum flow velocity, u for sliding as

$$u = \sqrt{\left(\frac{2\mu mg}{C_d A_n \rho_w}\right)}$$

where μ is the friction coefficient — following studies of boulders transported on basalt (Noormets et al., 2004) and sand-covered limestone platforms (Goto et al., 2007), the value $\mu = 0.7$ is used for the boulders transported at Lhok Nga and Satitoa. It should be noted that irregular micro-topography and other impediments to sliding would increase this friction coefficient. Non-negligible topographic slopes require the modification of the gravitational force term. m is the submerged boulder mass (kg). $m = V(\rho_p - \rho_w)$, where V (volume of the boulder) is equal to A*B*C (respectively length, width and thickness of the clast), ρ_p is the particle density calculated to be 2400 kg m^{-3} for the limestone boulders at Lhok Nga (Paris et al., 2009) and 2545 kg m^{-3} for the basalt boulders at Satitoa. An average boulder density was calculated from basalt boulders at Satitoa using four representative samples, whereby samples were weighed and fluid displacement used to measure the sample volume. g is acceleration due to gravity (9.81 m s^{-2}). C_d is the drag coefficient, taken as 1.5. A_n is the cross-sectional area (m^2) of the boulder normal to the flow and is equal to A*C, with the A-axis perpendicular to the flow and the C-axis vertical. ρ_w is the fluid density, taken as 1025 kg m^{-3}.

Balancing the resistance moment with the drag force moment and solving for flow velocity gives the minimum flow velocity for overturning,

$$u = \sqrt{\frac{l_g mg}{l_d 0.5 C_d A_n \rho_w}}$$

where l_g is the resistance moment arm equal to 0.5*B-axis length and l_d is the drag force moment arm equal to 0.5*C-axis length.

Table 3 gives the estimated tsunami flow velocities based on the characteristics of the largest boulders transported and deposited both offshore and inland, compared with flow velocities estimated after numerical modelling and eyewitness accounts. The range of distance from the shore is given for all observed boulders. Fig. 14 shows calculations of the minimum flow velocity for boulder transport at Lhok Nga, Sumatra (Fig. 14A) and Satitoa, Samoa (Fig. 14B). Lift and inertial forces on boulders are ignored in these calculations, but if they are significant, then minimum flow velocities will be lower. Minimum flow velocities calculated from boulders are compared with estimates from field measurements of flow depth for Froude numbers of 0.5, 1.0, and 1.5. The Froude number, Fr is a non-dimensional number that describes whether a flow is supercritical (>1), critical (=1), or subcritical (<1). The Froude number is equal to:

$$Fr = U / \sqrt{gh}$$

where U is the flow-speed, g is acceleration due to gravity and h is flow depth. The value for the Froude number for tsunamis varies spatially and temporally, but there is guidance on appropriate values to choose (Jaffe et al., 2011). Fritz et al. (2006) calculated Froude numbers ranging from 0.61 to 1.04 from Particle Image Velocimetry analysis of

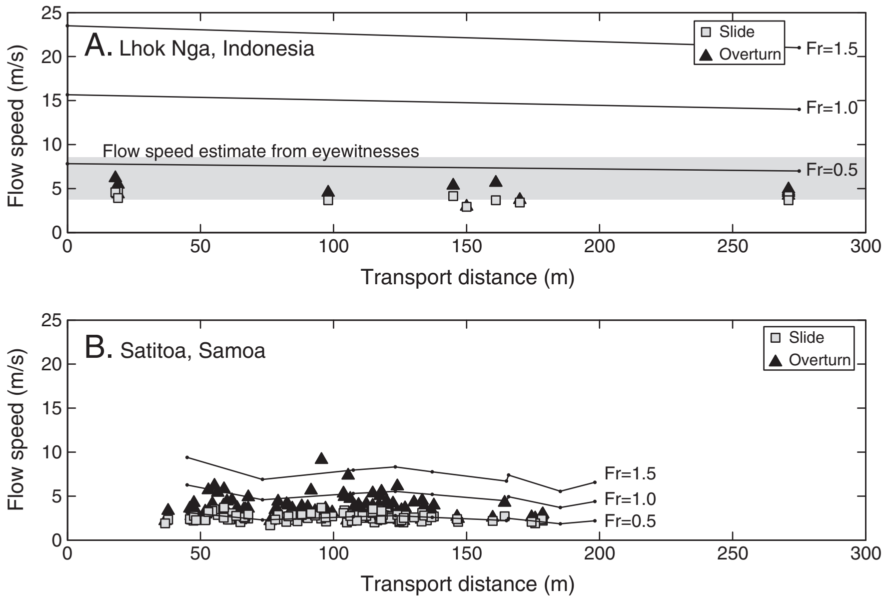

Fig. 14. Estimation of the minimum flow velocity for sliding and overturning of transported boulders at Lhok Nga, Sumatra (A) and Satitoa, Samoa (B). Flow velocity estimates are compared with flow velocities calculated from flow depth measurements considering various Froude numbers (Fr). The shaded flow velocity range (A) gives the flow velocity range estimated by Paris et al., 2009.

Author's personal copy

video imagery taken approximately 3 km inland in Banda Aceh during inundation by the 2004 IOT. Matsutomi et al. (2001) calculated Froude numbers of 0.7 to 2.0 for six tsunamis using velocities estimated using Bernoulli's principle applied to flow depths measured on the upstream (front) and downstream (rear) walls of houses, while Yeh (1991) calculated a Froude number of 1.43 for the leading edge of an experimental tsunami bore. Jaffe et al. (2011) have flow velocity estimates from inverse modelling (Huntington et al., 2007) using the sandy tsunami deposit at Satitoa, while Weiss and Fritz (2010) used small coral boulders on Savaii for their velocity estimates. Velocity estimates for the two sandy layers deposited by the tsunami waves in Satitoa are 3.8, 3.6, 3.7 m/s and 4.4, 4.4, 4.1 m/s at 100, 170, 240 m inland, respectively. They are very site specific and there were no direct measurements or video for Satitoa.

9. What can be learned from numerical models?

Lorang (2000) proposed equations predicting the threshold entrainment mass for a boulder beach during storms. Nott (1997) developed hydrodynamic equations to assess the pre-transport environment of a coastal boulder moved by tsunamis or storm surges, further specified for different initial positions of the boulders, such as submerged, subaerial and joint-bounded (Nott, 2003). Nott's equations, including the effect of drag, lift, inertia and buoyant forces to the boulder, were derived mainly by applying the moment of hydrodynamic forces to the boulder to predict whether the boulder would be overturned by the fluid impact. These equations have been used widely in previous studies (e.g. Mastronuzzi and Sansò, 2004; Scicchitano et al., 2007; Scheffers et al., 2008; Maouche et al., 2009). The ability to recognise the magnitude of extreme events in terms of hydraulic properties with this type of simple model using such parameters as the current velocity or water depth, would be useful in reconstructing pre-historic extreme events and preparing hazard maps for future scenarios (Pignatelli et al., 2009). Noormets et al. (2004) developed similar equations focusing on dislodgment, emplacement and transport of a boulder by the fluid force. These equations included additional components, such as tensile strength and crack forces based on the properties of rock and of friction between the boulder surface and the bed on which it moved. Imamura et al. (2008) on the other hand improved a practical model for boulder transport by tsunamis initially developed by Noji et al. (1993), which takes into account the various transport modes. They introduced an empirical variable coefficient of friction by assuming that this coefficient decreases with decrease in ground contact time when the boulder is transported by rolling or saltation. In addition they developed a two-dimensional numerical model which includes depth-averaged governing equations for the continuity and momentum of fluids plus the momentum equation for boulders (Imamura et al., 2001). Goto et al. (2010c) used this model to simulate boulder transport at Pakarang Cape, Thailand, during the 2004 IOT. However, despite significant advances in numerical modelling over the last decade the current numerical and empirical models available for the analysis of boulders do not definitively allow the differentiation of storm or tsunami transport based solely on the size of the boulders and their position in the landscape (Switzer and Burston, 2010).

Nott's 2003 equations were recently revised by Nandasena et al. (in press). The equation for the submerged boulder scenario was revised by rearranging the lift area of the lift force (Voropayev et al., 2001). The subaerial boulder scenario was revised by both rearranging the lift area and omitting the use of inertia force, and the joint-bounded scenario was revised by balancing force components in lifting directions. Slope at the pre-transport location is also taken in account by the revised equations. The minimum current velocity required to initiate the transport of submerged coral boulders from the revised equation is less than the result from Nott's equations (e.g. reduction up to 56% for submerged boulders, 65% for joint-bounded blocks). This difference is attributed to the increment of lift area in the revised equation. The minimum current velocity required to initiate the transport of subaerial boulders also varied from the result of Nott's equation (e.g. 4–22% less for boulders detached from the seawall in Lhok Nga). If we consider a joint-bounded scenario (e.g. tabular megaslabs in Lhok Nga), the minimum current velocity varies from −24% to +5% less when compared with the results from Nott's equation. The changes correspond to the increment in the lift force against the weight of the boulder and vice versa in the revised equation. Results from these revised equations are closer to velocities estimated by Paris et al. (2010).

In Samoa, numerical simulations show that the boulders are not transported by the first tsunami wave when the A-axis >1.0 m. In the numerical model, there is also no back-transport of boulders by backwash, which could be explained by a bed level that is lower than the coastal road and favours very slow return flow and water ponding (Movie 1). According to field measurements, some boulders (A-axis >1.0 m) were transported more than 100 m inland, however most of the numerical results are far less than those measured in the field, which is contrary to previous results in Lhok Nga (Nandasena et al., in press). As the simulation assumes a tabular shape for the boulders, boulder weight is greatly overestimated. This could explain why the model underestimates the transport distances because the larger the boulder weight, the higher the frictional resistance. Another reason could be inter-clast collisions although this is thought to be minimal. The model is one dimensional and simulates saltation and sliding but not rolling, even though many of the boulders could have been transported by rolling. The other reasons for the difference between the numerical results and the field measurements could be microtopography (simplified in the model) and coastal plain roughness (i.e. trees and buildings), not considered by the model.

10. Summary and conclusions

Coastal rip-rap revetments affected by an extreme wave offer the opportunity to study boulder transport inland. A comparison between the impacts of the 2009 SPT and 2004 IOT on two boulder rock armours shows similar characteristics, such as limited extent of landward transport and the absence of landward fining. The latter might be explained by inter-clast interaction/collision as, when a tsunami wave travels over a rocky platform it gradually incorporates boulder-sized clasts when available.

In both Satitoa and Lhok Nga, boulder concentrations occur in an area where the flow depth decreases abruptly. Flow velocity reduction occurs as the tsunami waves move overland but can vary significantly with changes in topography and increases in bed friction. Discrepancies between modelling and field data can therefore be related to how coefficients used in mathematical models simplify changes in coastal plain roughness (buildings, trees), microtopography, clast shape and boulder collision during transport.

How can we decipher the tsunami or storm origin for a boulder deposit? Differentiating between the two processes has been achieved by comparing the wave height required for boulder transport and the wave climate of a particular area (Scicchitano et al., 2007). Following Nott's 2003 equations, when the normal wave climate, including extreme storm waves, is insufficient to generate the minimum wave height needed, then large boulder deposits can be attributed to emplacement by tsunamis. Therefore these boulders are essentially tsunamigenic by default. This first approach is only relevant if the boulder transport mode (i.e. Nott's hydrodynamic equations) is correctly assessed.

Only large tsunamis have sufficient flow velocities to transport a large number of boulders from 15 to 25 m water depth offshore. We suggest that future studies coupling offshore–onshore mapping of boulder accumulations with reconstruction of the morphological history (sea-level variations, coastal sediment discharge and landform evolution) may allow researchers to distinguish between palaeostorm and palaeo-tsunami deposits.

Author's personal copy

Boulder deposits are often considered in isolation from other evidence related to their emplacement. While a tsunami deposit is source dependent, there is likely to be evidence for deposition of finer fractions such as gravel, sand and silt. The use of a multi-proxy approach to the study of palaeo-tsunami deposits offers the researcher the opportunity to use other contextual information to determine whether or not the sediments in question were deposited by tsunami or storm. These proxy data are not only geological, but also geomorphological, archaeological, anthropological and ecological (e.g. Goff et al., 2010b,c, 2011).

Appendix A. Supplementary data

Supplementary data to this article can be found online at doi:10.1016/j.earscirev.2010.12.006.

References

Ammon, C.J., Ji, C., Thio, H.-K., Robinson, D., Ni, S., Hrorleifsdottir, V., Kanamori, H., Lay, T., Das, S., Helmberger, D., Ichinose, G., Polet, J., Wald, D., 2005. Rupture process of the 2004 Sumatra-Andaman earthquake. Science 308, 1133–1139.

Bahlburg, H., Weiss, R., 2006. Sedimentology of the December 26, 2004 Sumatra tsunami deposits in eastern India (Tamil Nadu) and Kenya. International Journal of Earth Sciences 96 (6), 1195–1209.

Beavan, R.J., Wang, X., Holden, C., Wilson, K.J., Power, W.L., Prasetya, G., Bevis, M., Kautoke, R., 2010. Near-simultaneous great earthquakes at Tongan megathrust and outer rise in September 2009. Nature 466 (7309), 959–964.

Bevis, M., Taylor, F.W., Schutz, B.E., Recy, J., Isacks, B.L., Helu, S., Singh, R., Kendrick, E., Stowell, J., Taylor, B., Calmant, S., 1995. Geodetic observations of very rapid convergence and back-arc extension at the Tonga arc. Nature 374 (6519), 249–251.

Bourrouilh-Le Jan, F.G., Talandier, J., 1985. Sédimentation et fracturation de haute énergie en milieu récifal: tsunamis, ouragans et cyclones et leurs effets sur la sédimentologie de la géomorphologie d'un atoll: motu et hoa à Rangiroa, Tuamotu, SE Pacifique. Marine Geology 37, 263–272.

Buckley, M., Wei, Y., Jaffe, B., Watt, S., in press. Inverse modelling of velocities and inferred cause of overwash that emplaced inland fields of boulders at Anegada, British Virgin Islands. Natural Hazards.

Cailleux, A., Tricart, J., 1959. Contribution à l'étude des sables et des galets. CDU, Paris. 376 pp.

Cantalamessa, G., Di Celma, C., 2005. Sedimentary features of tsunami backwash deposits in a shallow marine Miocene setting, Mejillones Peninsula, northern Chile. Sedimentary Geology 178, 259–273.

Chlieh, M., Avouac, J.-P., Hjorleifsdottir, V., Song, T.-R.A., Sieh, K., Sladen, A., Hébert, H., Prawirodirdjo, L., Bock, Y., Galetzka, J., 2007. Coseismic slip and afterslip of the great (Mw 9.15) Sumatra–Andaman Earthquake of 2004. Bulletin. Seismological Society of America 97, 152–173.

Choi, B.H., Hone, S.J., Pelinovsky, E., 2006. Distribution of runup heights of the December 26, 2004 tsunami in the Indian Ocean. Geophysical Research Letters 33 (13), L13601.

Dawson, A.G., 1994. Geomorphological effects of tsunami run-up and backwash. Geomorphology 10, 83–94.

Dawson, A.G., Shi, S., Dawson, S., Takahashi, T., Shuto, N., 1996. Coastal sedimentation associated with the June 2nd and 3rd, 1994 tsunami in Rajegwesi, Java. Quaternary Science Review 15, 901–912.

de Lange, W.P., de Lange, P.J., Moon, V.G., 2006. Boulder transport by waterspouts: an example from Aorangi Island, New Zealand. Marine Geology 230, 115–125.

UNESCO-IOC International Tsunami Survey Team Samoa (ITST Samoa) Interim Report of Field Survey. In: Dominey-Howes, D., Thaman, R. (Eds.), 14th-21st October 2009. Australian Tsunami Research Centre Miscellaneous Report 2: October 2009. 190 pp.

Etienne, S., 2007. Les plates-formes rocheuses des littoraux volcaniques. In: Etienne, S., Paris, R. (Eds.), Les littoraux volcaniques: une approche environnementale. Presses Universitaires Blaise-Pascal, Clermont-Ferrand, pp. 37–55.

Etienne, S., Paris, R., 2010. Boulder accumulations related to storms on the Reykjanes Peninsula, Iceland. Geomorphology 114, 55–70.

Feldens, P., Schwarzer, K., Szczucinski, W., Stattegger, K., Sakuna, D., Somgpongchaiykul, P., 2009. Impact of the 2004 Indian Ocean tsunami on seafloor morphology and sediments offshore Pakarang Cape, Thailand. Polish Journal of Environmental Studies 18 (1), 63–68.

Felton, E.A., 2002. Sedimentology of rocky shorelines: 1. A review of the problem, with analytical methods, and insights gained from the Hulopoe Gravel and the modern rocky shoreline of Lanai, Hawaii. Sedimentary Geology 152, 221–245.

Felton, E.A., Crook, K.A.W., 2003. Evaluating the impacts of huge waves on rocky shorelines: an essay review of the book 'Tsunami — the underrated hazard'. Marine Geology 197, 1–12.

Fritz, H.M., Borrero, J.C., Synolakis, C.E., Yoo, J., 2006. 2004 Indian Ocean tsunami flow velocity measurements from survivor videos. Geophysical Research Letters 33, L24605.

Frohlich, C., Hornbach, M.J., Taylor, F.W., Shen, C.-C., Moala, A., Morton, A.E., Kruger, J., 2009. Huge erratic boulders in Tonga deposited by a prehistoric tsunami. Geology 37, 131–134.

Gelfenbaum, G., Jaffe, B., 2003. Erosion and sedimentation from the 17 July, 1998 Papua New Guinea tsunami. Pure and Applied Geophysics 160, 1969–1999.

Goff, J.R., Dudley, W.C., deMaintenon, M.J., Cain, G., Coney, J.P., 2006a. The largest local tsunami in 20th century Hawaii. Marine Geology 226, 65–79.

Goff, J., Liu, P., Higman, B., Morton, R., Jaffe, B., Fernando, H., Lynett, P., Fritz, H., Synolakis, C., Fernando, S., 2006b. Sri Lanka field survey after the December 2004 Indian Ocean tsunami. Earthquake Spectra 22, S155.

Goff, J., Nichol, S.L., Kennedy, D., 2010a. Development of a palaeotsunami database for New Zealand. Natural Hazards 54, 193–208. doi:10.1007/511069-009-9461-5.

Goff, J., Pearce, S., Nichol, S.L., Chagué-Goff, C., Horrocks, M., Strotz, L., 2010b. Multi-proxy records of regionally-sourced tsunamis, New Zealand. Geomorphology 118, 369–382. doi:10.1016/j.geomorph.2010.02.005.

Goff, J., Weiss, R., Courtney, C., Dominey-Howes, D., 2010c. Testing the hypothesis for tsunami boulder deposition from suspension. Marine Geology 277, 73–77. doi:10.1016/j.margeo.2010.08.003.

Goff, J., Lamarche, G., Pelletier, B., Chagué-Goff, C., Strotz, L., 2011. Palaeotsunami precursors to the 2009 South Pacific tsunami in the Wallis and Futuna archipelago. Earth-Science Reviews 107, 90–105 (this issue).

Goto, K., Imamura, F., 2007. Numerical models for sediment transport by tsunamis. The Quaternary Research (Daiyonki-Kenkyo) 46, 463–475.

Goto, K., Chavanich, S.A., Imamura, F., Kunthasap, P., Matsui, T., Minoura, K., Sugawara, D., Yanagisawa, H., 2007. Distribution, origin and transport process of boulders deposited by the 2004 Indian Ocean tsunami at Pakarang Cape, Thailand. Sedimentary Geology 202, 821–837.

Goto, K., Okada, K., Imamura, F., 2009. Characteristics and hydrodynamics of boulders transported by storm wave at Kudaka Island, Japan. Marine Geology 262, 14–24.

Goto, K., Miyagi, K., Kawamata, H., Imamura, F., 2010a. Discrimination of boulders deposited by tsunamis and storm waves at Ishigaki Island, Japan. Marine Geology 269, 34–45.

Goto, K., Okada, K., Imamura, F., 2010b. Numerical analysis of boulder transport by the 2004 Indian Ocean tsunami at Pakarang Cape, Thailand. Marine Geology 268, 97–105.

Goto, K., Kawana, T., Imamura, F., 2010c. Historical and geological evidence of boulders deposited by tsunamis, southern Ryukyu Islands, Japan. Earth Science Reviews 102, 77–99.

Hall, A.M., Hansom, J.D., Williams, D.M., Jarvis, J., 2006. Distribution, geomorphology and lithofacies of cliff-top storm deposits: examples from the high-energy coasts of Scotland and Ireland. Marine Geology 232, 131–155.

Hall, A.M., Hansom, J.D., Jarvis, J., 2008. Patterns and rates of erosion produced by high energy wave processes on hard rock headlands: The Grind of the Navir, Shetland, Scotland. Marine Geology 248, 28–46.

Hall, A.M., Hansom, J.D., Williams, D.M., 2010. Wave-emplaced coarse debris and megaclasts in Ireland and Scotland: boulder transport in high-energy littoral environment: a discussion. Journal of Geology 118, 699–704.

Hansom, J.D., Hall, A.M., 2009. Magnitude and frequency of extra-tropical North-Atlantic cyclones: a chronology from cliff-top storm deposits. Quaternary International 195, 42–52.

Hearty, P., 1997. Boulder deposits from large waves during the last interglaciation on north Eleuthera Island, Bahamas. Quaternary Research 48, 326–338.

Hori, K., Kuzumoto, R., Hirouchi, D., Umitsu, M., Janjirawuttikul, N., Patanakanog, B., 2007. Horizontal and vertical variations of 2004 Indian tsunami deposits: an example of two transects along the western coast of Thailand. Marine Geology 239, 163–172.

Huntington, K., Bourgeois, J., Gelfenbaum, G., Lynett, P., Yeh, H., Jaffe, B., Weiss, R., 2007. Sandy signs of a tsunami's onshore depth and speed. EOS. Transactions of the American Geophysical Union 88 (52), 577–578.

Hyvernaud, O., 2009. Dislocations des barrières récifales occasionnées par un cyclone de forte énergie. 11th Pacific Science Inter-Congress, Tahiti.

Imamura, F., Yoshida, I., Moore, A., 2001. Numerical study of the 1771 Meiwa tsunami at Ishigaki Island, Okinawa and the movement of the tsunami stones. Proceedings Coastal Engineering, JSCE 48, 346–350.

Imamura, F., Goto, K., Ohkubo, S., 2008. A numerical model of the transport of a boulder by tsunami. Journal of Geophysical Research 113, C01008.

Jaffe, B.E., Gelfenbaum, G., 2007. A simple model for calculating tsunami flow-speed from tsunami deposits. Sedimentary Geology 200, 347–361.

Jaffe, B., Buckley, M., Richmond, B., Strotz, L., Etienne, S., Clark, K., Gelfenbaum, G., 2011. Grading and inverse modeling of sandy tsunami deposits to estimate flow speed during the 29 September 2009 tsunami near Satitoa, east Upolu, Samoa. Earth-Science Reviews 107, 22–36 (this issue).

Kelletat, D., Scheffers, A., Scheffers, S., 2004. Holocene tsunami deposits on the Bahaman Islands of Long Island and Eleuthera. Zeitschrift für Geomorphologie 48, 519–540.

Kelletat, D., Scheffers, S.R., Scheffers, A., 2007. Field signatures of the SE-Asian megatsunami along the West Coast of Thailand compared to Holocene paleotsunami from the Atlantic region. Pure and Applied Geophysics 164, 413–431.

Laboute, P., 1985. Evaluation of damage done by the cyclones of 1982–1983 to the outer slope of the Tikehau and Takapoto atolls (Tuamotu archipelago). Proceedings of the fifth international coral reef congress, Tahiti, vol. 3 — Symposia and Seminars (A), pp. 323–329.

Lamarche, G., Pelletier, B., Goff, J., 2010. The 29 September 2009 South Pacific Tsunami in Wallis and Futuna. Marine Geology 271, 297–302.

Lavigne, F., Paris, R., Grancher, D., Wassmer, P., Brunstein, D., Vautier, F., Leone, F., Flohic, F., De Coster, B., Gunawan, T., Gomez, Ch., Setiawan, A., Cahyadi, R., Fachrizal, 2009. Reconstruction of tsunami inland propagation on December 26, 2004 in Banda Aceh, Indonesia, through field investigations. Pure and Applied Geophysics 166, 259–281.

Lay, T., Ammon, C.J., Kanamori, H., Rivera, L., Koper, K.D., Hutko, A.R., 2010. The 2009 Samoa-Tonga great earthquake triggered doublet. Nature 466 (7309), 964–968.

Author's personal copy

Le Roux, J.P., Vargas, G., 2005. Hydraulic behavior of tsunami backflows: insight from their modern and ancient deposits. Environmental Geology 49, 65–75.

Le Roux, J.P., Gómez, C., Fenner, J., Middleton, H., 2004. Sedimentological processes in a scarp-controlled rocky shoreline to upper continental slope environment, as revealed by unusual sedimentary features in the Neogene Coquimbo Formation, north-central Chile. Sedimentary Geology 165, 67–92.

Lorang, M., 2000. Predicting the threshold entrainment mass for a boulder. Journal of Coastal Research 16, 432–445.

Loevenbruck, A., Hebert, H., Schindele, F., Sladen, A., Lavigne, F., Brunstein, D., Wassmer, P., Paris, R., 2007. Detailed Modeling of the 2004 Tsunami Flooding in the Banda Aceh and Lhok Nga Districts (Sumatra, Indonesia). American Geophysical Union, Fall Meeting 2007, abstract #S53A-1042.

Maeno, F., Imamura, F., 2007. Numerical investigations of tsunamis generated by pyroclastic flows from the Kikai caldera, Japan. Geophysical Research Letters 34, L23303. doi:10.1029/2007GL031222.

Maouche, S., Morhange, C., Meghraoui, M., 2009. Large boulder accumulation on the Algerian coast evidence tsunami events in the western Mediterranean. Marine Geology 262, 96–104.

Mastronuzzi, G., Sansò, P., 2000. Boulders transport by catastrophic waves along the Ionian coast of Apulia (southern Italy). Marine Geology 170, 93–103.

Mastronuzzi, G., Sansò, P., 2004. Large boulder accumulations by extreme waves along the Adriatic coast of southern Apulia (Italy). Quaternary International 120, 173–184.

Matsutomi, H., Shuto, N., Imamura, F., Takhashi, T., 2001. Field survey of the 1996 Irian Jaya Earthquake tsunami in Biak Island. Natural Hazards 24, 199–212.

McKenna, J., 1990. Morphodynamics and sediments of basalt shore platforms. Unpubl. PhD thesis, University of Ulster, Coleraine, 2 vols, 348 pp and 234 pp.

McMurtry, G.M., Fryer, G.J., Tappin, D.R., Wilkinson, I.P., Williams, M., Fietzke, J., Garbe-Schoenberg, D., Watts, P., 2004. Megatsunami deposits on Kohala volcano, Hawaii, from flank, collapse of Mauna Loa. Geology 32 (9), 741–744.

Meltzner, A.J., Sieh, K., Abrams, M., Agnew, D.-C., Hudnut, K.-W., Avouac, J.-P., Natawidjaja, D.H., 2006. Uplift and subsidence associated with the great Aceh-Andaman earthquake of 2004. Journal of Geophysical Research 111, B02407.

Minoura, K., Imamura, F., Takahashi, T., Shuto, N., 1997. Sequence of sedimentation processes caused by the 1992 Flores tsunami: evidence from Babi Island. Geology 25, 523–526.

Moore, J.G., Moore, G.W., 1984. Deposit from a giant wave on the island of Lanai, Hawaii. Science 226, 1312–1315.

Morton, R.A., Richmond, B.M., Jaffe, B.E., Gelfenbaum, G., 2006. Reconnaissance investigation of Caribbean extreme wave deposits — preliminary investigations, interpretations, and research directions. Open-File Report 2006–1293. USGS. 41 pp.

Morton, R.A., Goff, J.R., Nichol, S.L., 2008. Hydrodynamic implications of textural trends in sand deposits of the 2004 tsunami in Sri Lanka. Sedimentary Geology 207 (1–4), 56–64.

Mulder, T., Alexander, J., 2001. The physical character of subaqueous sedimentary density flows and their deposits. Sedimentology 48, 269–299.

Nandasena, N.A.K., Paris, R., Tanaka, N., in press. Numerical assessment of boulder transport by the 2004 Indian Ocean tsunami in Lhok Nga, West Bandah Aceh (Sumatra, Indonesia). Computers and Geosciences.

Noda, A., Katayama, H., Sagayama, T., Suga, K., Uchida, Y., Satake, K., Abe, K., Okamura, Y., 2007. Evaluation of tsunami impacts on shallow marine sediments: an example from the tsunami caused by the 2003 Tokachi-oki earthquake, Northern Japan. Sedimentary Geology 200, 314–327.

Noji, M., Imamura, F., Shuto, N., 1993. Numerical simulation of movement of large rocks transported by tsunamis. Proceedings of IUGG/IOC International Tsunami Symposium, pp. 189–197.

Noormets, R., Felton, E.A., Crook, K.A.W., 2002. Sedimentology of rocky shorelines: 2. Shoreline megaclasts on the north shore of Oahu, Hawaii — origins and history. Sedimentary Geology 150, 31–45.

Noormets, R., Crook, K.A.W., Felton, E.A., 2004. Sedimentology of rocky shorelines: 3. Hydrodynamics of megaclast emplacement and transport on a shore platform, Oahu, Hawaii. Sedimentary Geology 172, 41–65.

Nott, J., 1997. Extremely high wave deposits inside the Great Barrier Reef, Australia: determining the cause-tsunami or tropical cyclone. Marine Geology 141, 193–207.

Nott, J., 2003. Waves, coastal boulder deposits and the importance of the pre-transport setting. Earth and Planetary Science Letters 210, 269–276.

Oak, H.L., 1984. The boulder beach: a fundamentally distinct sedimentary assemblage. Annals of the Association of American Geographers 74, 71–82.

Onda, M., 1999. The distribution of large reef blocks and the effect of geomorphic development in Kudaka Island, the Ryukyu Islands, Japan. Geographical Review Japan 72A–11, 746–762.

Paris, R., Pérez Torrado, F.J., Cabrera, M.C., Schneider, J.L., Wassmer, P., Carracedo, J.C., 2004. Tsunami-induced conglomerates and debris flow deposits on the western coast of Gran Canaria (Canary Islands). Acta Vulcanologica 16 (1), 133–136.

Paris, R., Lavigne, F., Wassmer, P., Sartohadi, J., 2007. Coastal sedimentation associated with the December 26, 2004 tsunami in Lhok Nga, west Banda Aceh (Sumatra, Indonesia). Marine Geology 238, 93–106.

Paris, R., Wassmer, P., Sartohadi, J., Lavigne, F., Barthomeuf, B., Desgages, E., Grancher, D., Baumert, P., Vautier, F., Brunstein, D., Gomez, C., 2009. Tsunamis as geomorphic crises: Lessons from the December 26, 2004 tsunami in Lhok Nga, West Banda Aceh (Sumatra, Indonesia). Geomorphology 104, 59–72.

Paris, R., Fournier, J., Poizot, E., Etienne, S., Morin, J., Lavigne, F., Wassmer, P., 2010. Boulder and fine sediment transport and deposition by the 2004 tsunami in Lhok Nga (western Banda Aceh, Sumatra, Indonesia): a coupled offshore — onshore model. Marine Geology 268, 43–54.

Pérez Torrado, F.J., Paris, R., Cabrera, M.C., Schneider, J.L., Wassmer, P., Carracedo, J.C., Rodriguez Santana, A., Santana, F., 2006. The Agaete tsunami deposits (Gran Canaria): evidence of tsunamis related to flank collapses in the Canary Islands. Marine Geology 227, 137–149.

Pignatelli, C., Sanso, P., Mastronuzzi, G., 2009. Evaluation of tsunami flooding using geomorphologic evidence. Marine Geology 260, 6–18.

Razzhigaeva, N.G., Ganzei, L.A., Grebennikova, T.A., Ivanova, E.D., Kaistrenko, V.M., 2006. Sedimentation particularities during the tsunami of December 26, 2004, in northern Indonesia: Simelue Island and the Medan coast of Sumatra Island. Oceanology 46 (6), 875–890. doi:10.1134/S000143700606013.

Richmond, B.M., Morton, R.A., 2007. Coral-gravel storm ridges: examples from the tropical Pacific and Caribbean. Proceedings Coastal Sediments 2007, 572–583.

Richmond B.M., Watt S., Buckley M., Jaffe B.E., Gelfenbaum G., Morton R.A., in press. Recent storm and tsunami deposit characteristics, Southeast Hawai'i. Marine Geology, doi:10.1016/j.margeo.2010.08.001.

Richmond, B., Buckley, M., Etienne, S., Strotz, L., Chagué-Goff, C., Clark, K., Goff, J., McAdoo, B., 2011. Geologic signatures of the September 2009 South Pacific tsunami in the Samoan Islands. Earth Science Reviews 107, 37–50 (this issue).

Ruellan, E., Lagabrielle, Y., 2005. Subductions et ouvertures océaniques dans le Sud-Ouest du Pacifique. Géomorphologie: Relief, Processus, Environnement 2, 121–142.

Sato, H., Shimamoto, T., Tsutsumi, A., Kawamoto, E., 1995. Onshore tsunami deposits caused by the 1993 Southwest Hokkaido and 1983 Japan Sea earthquakes. Pure and Applied Geophysics 144, 693–717.

Scheffers, A., 2004. Tsunami imprints on the Leeward Netherlands Antilles (Aruba, Curaçao, Bonaire) and their relation to other coastal problems. Quaternary International 120, 163–172.

Scheffers, A., 2005. Coastal response to extreme wave events — hurricanes and tsunami on Bonaire. Essener Geographische Arbeiten 37 100 pp.

Scheffers, A., Kelletat, D., 2003. Sedimentologic and geomorphologic tsunami imprints worldwide — a review. Earth Science Reviews 63, 83–92.

Scheffers, A., Scheffers, S.R., 2007. First significant tsunami evidence from historical times in western Crete (Greece). Earth and Planetary Science Letters 259 (3-4), 613–624.

Scheffers, A., Kelletat, D., Vött, A., May, S.M., Scheffers, S., 2008. Large Holocene tsunami traces on the western and southern coastlines of the Peloponnesus (Greece). Earth and Planetary Science Letters 269, 271–279.

Scheffers, A., Scheffers, S., Kelletat, D., Browne, T., 2009. Wave-emplaced coarse debris and megaclasts in Ireland and Scotland: boulder transport in high-energy littoral environment. Journal of Geology 117, 553–573.

Scheffers, A., Kelletat, D., Scheffers, S., 2010. Wave-emplaced coarse debris and megaclasts in Ireland and Scotland: boulder transport in high-energy littoral environment: a reply. Journal of Geology 118, 705–709.

Scicchitano, G., Monaco, C., Tortorici, L., 2007. Large boulder deposits by tsunami waves along the Ionian coast of south-eastern Sicily (Italy). Marine Geology 238, 75–91.

Shi, S., Dawson, A.G., Smith, D.E., 1995. Coastal sedimentation associated with the December 12th, 1992 tsunami in Flores, Indonesia. Pure and Applied Geophysics 144, 525–536.

Shiki, T., Yamazaki, T., 1996. Tsunami-induced conglomerates in Miocene upper bathyal deposits, Chita Peninsula, central Japan. Sedimentary Geology 104, 175–188.

Smith, A.M., Mather, A.A., Bundy, S.C., Cooper, J.A.G., Guastella, L.A., Ramsay, P.J., Theron, A., 2010. Contrasting styles of swell-driven coastal erosion: examples from KwaZulu-Natal, South Africa. Geological Magazine 147, 940–953.

Spiske, M., Böröcz, Z., Bahlburg, H., 2008. The role of porosity in discriminating between tsunami and hurricane emplacement of boulders — a case study from the Lesser Antilles, southern Caribbean. Earth and Planetary Science Letters 268, 384–396.

Suanez, S., Fichaud, B., Magne, R., 2009. Cliff-top storm deposits on Banneg Island, Brittany, France: Effects of giant waves in the Eastern Atlantic Ocean. Sedimentary Geology 220, 12–28.

Subarya, C., Chlieh, M., Prawirodirdjo, L., Avouac, J.P., Bock, Y., Sieh, K., Meltzner, A.J., Natawidjaja, D.H., McCaffery, R., 2006. Plate-boundary deformation associated with the great Sumatra–Andaman earthquake. Nature 440, 46–51.

Sunamura, T., 1992. Geomorphology of rocky coasts. Wiley, Chichester. 302 pp.

Switzer, A.D., Burston, J.M., 2010. Competing mechanisms for boulder deposition on the southeast Australian coast. Geomorphology 114, 42–54.

Talandier, J., Bourrouilh-Le Jan, F., 1987. High energy sedimentation in French Polynesia: cyclone or tsunami? In: El-Sabh, M.I., Murty, T.S. (Eds.), Natural and man-made hazards. Reidel Publishing, pp. 181–187.

Tanner, L.H., Calvari, S., 2004. Unusual sedimentary deposits on the SE side of Stromboli volcano, Italy: products of a tsunami caused by the ca. 5000 BP Sciarra del Fuoco collapse? Journal of Volcanology and Geothermal Research 137, 329–340.

Terry, J.P., 2007. Tropical cyclones. Climatology and impacts in the South Pacific. Springer, New York. 210 pp.

Umitsu, M., Tanavud, C., Patanakanog, B., 2007. Effects of landforms on tsunami flow in the plains of Banda Aceh, Indonesia, and Nam Khem, Thailand. Marine Geology 242, 141–153.

Verbeek, R.D.M., 1886. Krakatau. Batavia. 567 pp.

Voropayev, S.I., Cense, A.W., McEachern, G.B., Boyer, D.L., Fernando, H.J.S., 2001. Dynamics of cobbles in the shoaling region of a surf zone. Ocean Engineering 28 (7), 763–788.

Weiss, R., Fritz, H., 2010. Boulders moved by the 29 September 2009 tsunami: flow-speed estimates at Taga, Samoa. Geophysical Research Abstracts 12 EGU2010-14277 http://meetingorganizer.copernicus.org/EGU2010/EGU2010-14277.pdf.

Whelan, F., Kelletat, D., 2005. Boulder deposits on the southern Spanish Atlantic coast: possible evidence for the 1755 AD Lisbon tsunami? Science of Tsunami Hazards 23, 25–38.

Williams, D.M., Hall, A.M., 2004. Cliff-top megaclasts deposits of Ireland, a record of extreme waves in the North Atlantic — storms or tsunamis? Marine Geology 206, 101–117.

Yeh, H.H., 1991. Tsunami bore runup. Natural Hazards 4, 209–220.